ELSEVIER

Journal of Alloys and Compounds 384 (2004) 67–70

Journal of ALLOYS AND COMPOUNDS

www.elsevier.com/locate/jallcom

Structural stability and electrical properties of $Sr_2Fe_{1+x}Mo_{1-x}O_{6-\delta}$ under high pressure

J.S. Zhang [a,b], R.C. Yu [a,*], P. E [a], F.Y. Li [a], X.D. Li [c], J. Liu [c], C.G. Feng [b], C.Q. Jin [a]

[a] *Institute of Physics, Chinese Academy of Sciences, P.O. Box 603, Beijing 100080, China*
[b] *School of Mechano-Electronics Engineering, Beijing Institute of Technology, Beijing 100081, China*
[c] *Institute of High Energy Physics, Chinese Academy of Sciences, Beijing 100039, China*

Received 26 February 2004; received in revised form 6 April 2004; accepted 6 April 2004

Abstract

Fe-substituted materials $Sr_2Fe_{1+x}Mo_{1-x}O_{6-\delta}$ ($x = 0$, 0.1, 0.2, 0.3, 0.4) were synthesized by a modified polymer-network gel method at a relatively low temperature. The structural stability and electrical properties of Sr_2FeMoO_6 and $Sr_2Fe_{1.4}Mo_{0.6}O_{6-\delta}$ have been studied using energy dispersive X-ray diffraction with synchrotron radiation and resistance and capacitance measurements, respectively. The results show that the crystal structure of $Sr_2Fe_{1.4}Mo_{0.6}O_{6-\delta}$ is as stable as Sr_2FeMoO_6 at high pressure and more compressible than Sr_2FeMoO_6. On the basis of the measurements of resistance and capacitance versus pressure, it is considered that they all undergo an electronic structure transition under high pressure.

Keywords: Double perovskite; Magnetoresistance; Polymer; High pressure

1. Introduction

Since the discovery of the colossal magnetoresistance (CMR) in doped perovskite manganates, much attention has been paid to their magnetic and electrical properties. For magnetic recording devices, large MR at low fields and over a wide temperature range would be desirable. Recently, the low field intergrain tunneling magnetoresistance (IMR) has been observed in a polycrystalline sample of the compound Sr_2FeMoO_6, with a Curie temperature as high as 410–450 K [1,2]. Due to the promising application of the CMR effect at room temperature, efforts have been made to investigate Ca_2FeMoO_6, Ba_2FeMoO_2 and $Sr_{2-x}Ba_xMoO_6$, which have a structure similar to that of Sr_2FeMoO_6 [3,4]. Sr_2FeMoO_6 consists of FeO_6 and MoO_6 octahedra arranged alternately in the lattice, forming an ordered double perovskite structure. Band structure calculations [1,5] predict that Sr_2FeMoO_6 has a half-metallic band structure where the conduction electrons are highly spin polarized even at room temperature. Because of the highly polarized Fermi-level electrons, the hopping of the carrier across intergrain depends sensitively on the spin scattering at the grain boundaries or the magnetic domain walls which can be suppressed by an external magnetic field [4,6]. In a general way, the ferromagnetic structure of Sr_2FeMoO_6 can be described as an ordered array of parallel Fe^{3+} magnetic moments, antiferromagnetically coupled with parallel Mo^{5+} spins [7]. As a rule of thumb, some properties of the materials, such as the electronic configuration, the phase structure, and the magnetic structure, are generally affected by the synthesis or the annealing processes [8,9]. The traditional solid state reaction [1] is usually performed at elevated temperatures, easily leading to by-products or structural inhomogeneities. To some extent, such disadvantages impose limitations on the applications and properties of the materials. In the present paper, we have successfully synthesized a series of the $Sr_2Fe_{1+x}Mo_{1-x}O_{6-\delta}$ compounds ($x = 0$, 0.1, 0.2, 0.3, 0.4) by a modified polymer-network gel method at a relatively low temperature. Also, the structural stability and the electrical properties of some products were investigated under high pressures considering that high pressure could modify the structural, electrical and magnetic properties of the samples.

* Corresponding author. Tel.: +86-10-82649159; fax: +86-10-82649531.
E-mail address: rcyu@aphy.iphy.ac.cn (R.C. Yu).

0925-8388/$ – see front matter © 2004 Elsevier B.V. All rights reserved.
doi:10.1016/j.jallcom.2004.04.089

2. Experimental details

Polycrystalline $Sr_2Fe_{1+x}Mo_{1-x}O_{6-\delta}$ ($x = 0$, 0.1, 0.2, 0.3, 0.4) powders were prepared by a modified polymer-network gel method in much the same way described in the literatures [10,11]. According to the formula $Sr_2Fe_{1+x}Mo_{1-x}O_{6-\delta}$, stoichiometric amounts of $Fe(NO_3)_3{\cdot}9H_2O$, $Sr(NO_3)_2$ and $(NH_4)_6Mo_7O_{24}{\cdot}4H_2O$ were dissolved in deionized water containing citric acid, forming a uniform solution. After the pH value was regulated with ammonia, polymerization agents and starters were added to the solution. Keeping the temperature at 80 °C for a few minutes, the solution polymerized into polymer gel. The gel was crushed, dried at 120 °C, then fired at 500 °C in an oxygen atmosphere to convert the gel into superfine powder. Finally, the powder was pelletized, heated at 700 °C for 6 h in a mixed gas stream of 1% H_2/Ar and then left to cool to room temperature to yield a product.

The crystal structure and phase purity of the samples were examined with a M18AHF diffractometer using Cu Kα radiation. The morphology of the samples was taken with an XL30 S-FEG scanning electron microscope (SEM). Energy dispersive X-ray diffraction experiments in situ high pressure on Sr_2FeMoO_6 and $Sr_2Fe_{1.4}Mo_{0.6}O_{6-\delta}$ were carried out in a diamond anvil cell (DAC), with a culet of 480 μm diameter, using synchrotron white radiation at the Beijing Synchrotron Radiation Facility (BSRF). The size of X-ray spot was 80 μm × 80 μm, and the diffraction angle (θ) was 7.0525 and 7.0558° for Sr_2FeMoO_6 and $Sr_2Fe_{1.4}Mo_{0.6}O_{6-\delta}$, respectively. The powder of the sample, together with an adequate amount of Au powder for internal calibration, was loaded into a 300 μm diameter hole in a T301 stainless-steel gasket. The unit cell volume ratio V/V_0 as a function of pressure P was calculated from the interplanar spacing under different pressures. We also measured the high pressure resistance and capacitance of the sample in a DAC, and the techniques used for DAC and measurements were the same as those reported previously [12]. The distance between the two molybdenum electrodes was set to be 0.03–0.05 mm, and the resistance and capacitance were recorded on a ZL5 intelligent inductance–capacitance–resistance (LCR) meter at 1 kHz. All the samples were pre-pressed under a pressure of about 4 GPa to make them compact before the experiment.

3. Results and discussion

The X-ray powder diffraction patterns of nano-scale polycrystalline $Sr_2Fe_{1+x}Mo_{1-x}O_{6-\delta}$ ($x = 0$, 0.1, 0.2, 0.3, 0.4) are plotted in Fig. 1. It shows a clean single phase without detectable secondary phase. The diffraction peaks are indexed to a tetragonal structure with a space group *I*4/*mmm*. The lattice parameters are refined from XRD data, and are listed in Table 1. As can be seen from Table 1, the lattice parameters of all the samples are very close to each other, similar to the result of the bulk sample with micrometer scale grain size [13], but present a slight decrease with increasing substitution of Fe for Mo, which can be explained by the fact that the radius of Fe^{3+} (0.66 Å) is a little smaller than that of Mo^{5+} (0.67 Å), but they are almost equivalent to each other. Fig. 2 shows the SEM images of Sr_2FeMoO_6

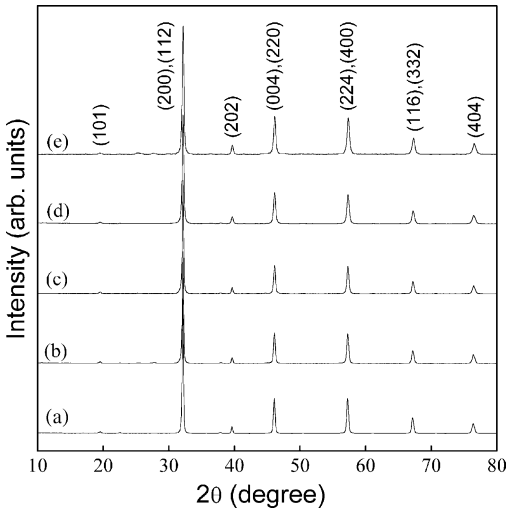

Fig. 1. The XRD patterns of the $Sr_2Fe_{1+x}Mo_{1-x}O_{6-\delta}$ (a) $x = 0$; (b) $x = 0.1$; (c) $x = 0.2$; (d) $x = 0.3$; (e) $x = 0.4$.

Table 1
The unit cell parameters of $Sr_2Fe_{1+x}Mo_{1-x}O_{6-\delta}$

Samples	a (nm)	c (nm)	V (nm^3)
Sr_2FeMoO_6	0.55665	7.8799	0.24417
$Sr_2Fe_{1.1}Mo_{0.9}O_{6-\delta}$	0.55651	7.8784	0.24400
$Sr_2Fe_{1.2}Mo_{0.8}O_{6-\delta}$	0.55624	7.8761	0.24369
$Sr_2Fe_{1.3}Mo_{0.7}O_{6-\delta}$	0.55618	7.8729	0.24353
$Sr_2Fe_{1.4}Mo_{0.6}O_{6-\delta}$	0.55604	7.8662	0.24321

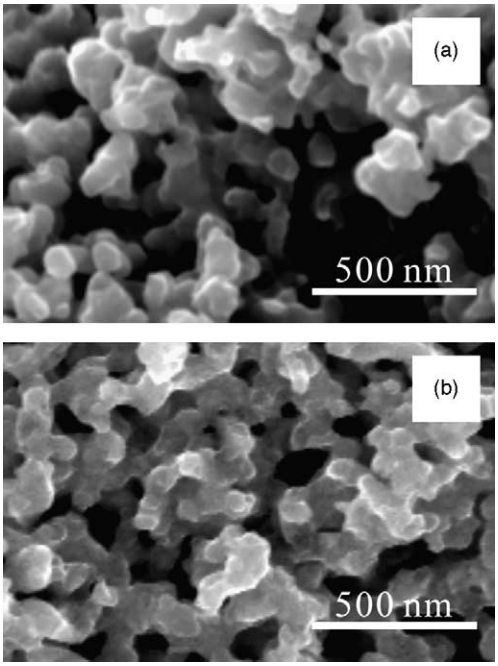

Fig. 2. SEM images of (a) Sr_2FeMoO_6 and (b) $Sr_2Fe_{1.4}Mo_{0.6}O_{6-\delta}$.

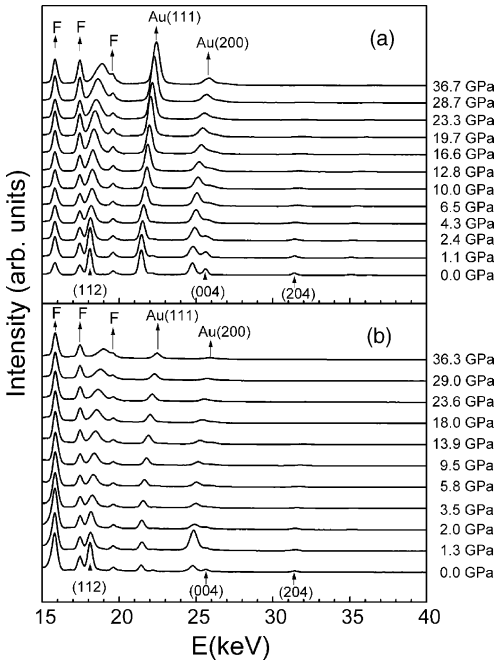

Fig. 3. In situ high pressure energy dispersive X-ray diffraction patterns of (a) Sr_2FeMoO_6 and (b) $Sr_2Fe_{1.4}Mo_{0.6}O_{6-\delta}$ at different pressures.

and $Sr_2Fe_{1.4}Mo_{0.6}O_{6-\delta}$. It can be clearly seen that the grain sizes of the two samples are about 100 nm, and the particles appear uniform and fine in the field of vision.

The in situ high pressure energy dispersive X-ray diffraction patterns of the Sr_2FeMoO_6 and $Sr_2Fe_{1.4}Mo_{0.6}O_{6-\delta}$ are presented in Fig. 3. The pressure ranges from 0 to 36.7 GPa and to 36.3 GPa for Sr_2FeMoO_6 and $Sr_2Fe_{1.4}Mo_{0.6}O_{6-\delta}$, respectively. Evidently, the change and trend of the patterns of $Sr_2Fe_{1.4}Mo_{0.6}O_{6-\delta}$ is similar to that of Sr_2FeMoO_6 as well as to that reported previously [13]. Fig. 3 shows that the sample peaks shift to higher energy with increasing pressure, which is caused by compression of the unit cell under high pressure. In addition, all the diffraction peaks weaken gradually with the increase of pressure because of some sample flowing out of the sample chamber with pressure. It is apparent that the sample peaks become broadened with increasing pressure. This may be caused by the fact that a gradient pressure on the sample leads to a gradient distribution of the interplanar spacing, and thus the peak broadens accordingly. When the pressure was released, the sample peaks were restored to the original positions and patterns. In addition to sample peaks and Au peaks, some fluorescence peaks (marked by F) of the elements in the sample appear in the patterns, but they do not change their position with pressure since the pressure we used is too low to change the energy levels of electron shells and sub-shells. It is noteworthy that in the pressure range considered here, no new diffraction peaks appeared and no diffraction peaks disappear in the patterns, suggesting that the crystal structure of the nano-scale Sr_2FeMoO_6 and $Sr_2Fe_{1.4}Mo_{0.6}O_{6-\delta}$ is stable. These results indicate that under high pressure, the structural stability of

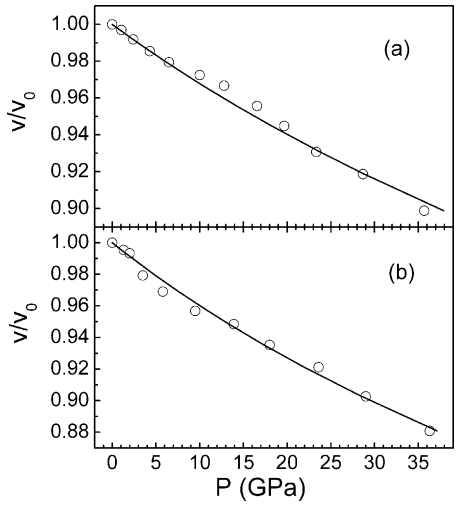

Fig. 4. V/V_0–P relationships for (a) Sr_2FeMoO_6 and (b) $Sr_2Fe_{1.4}Mo_{0.6}O_{6-\delta}$. The open circles represent the experimental data and the solid lines represent the fitting curves.

the substituted nano-scale $Sr_2Fe_{1.4}Mo_{0.6}O_{6-\delta}$ is similar to that of the parent compound Sr_2FeMoO_6.

On the basis of in situ high pressure energy dispersive X-ray diffraction, the cell parameters and volumes were calculated at each pressure and the V/V_0–P curves for the Sr_2FeMoO_6 and $Sr_2Fe_{1.4}Mo_{0.6}O_{6-\delta}$ are plotted in Fig. 4. Then the experimental data are fitted by the Birch–Murnaghan (B–M) equation:

$$P = \frac{3}{2}B_0\left[\left(\frac{V}{V_0}\right)^{-7/3} - \left(\frac{V}{V_0}\right)^{-5/3}\right] \times \left\{1 - \frac{3}{4}(4 - B_0') \times \left[\left(\frac{V}{V_0}\right)^{-2/3} - 1\right]\right\}$$

Assuming the first-order derivative to be equal to $B_0' = 4$, the bulk modulus B_0 was simulated to be 284 ± 6 and 227 ± 4 GPa for Sr_2FeMoO_6 and $Sr_2Fe_{1.4}Mo_{0.6}O_{6-\delta}$, respectively, i.e. the B_0 value of $Sr_2Fe_{1.4}Mo_{0.6}O_{6-\delta}$ is smaller than that of Sr_2FeMoO_6. This behavior is in agreement with the explanation that substitution of the smaller Fe^{3+} for Mo^{5+} and the existence of oxygen defects give rise to more space in the lattice, making $Sr_2Fe_{1.4}Mo_{0.6}O_{6-\delta}$ more compressible than Sr_2FeMoO_6. In general, a crystal structure transition or an electronic structure transition would affect the electrical properties of materials. In order to understand the effect of pressure on the electrical properties of the products, we measured the pressure dependent resistance and capacitance of the samples. Fig. 5 presents the pressure dependence of resistance (R–P) and capacitance (C–P) for Sr_2FeMoO_6 and $Sr_2Fe_{1.4}Mo_{0.6}O_{6-\delta}$, respectively. For Sr_2FeMoO_6, Fig. 5(a), the resistance remains unchanged at first, and then drops steeply at about 2.5 GPa, and decreases slowly up to 20 GPa. In response to R–P curve, the capacitance of Sr_2FeMoO_6 rises abruptly also at about 2.5 GPa and then changes very little with further increasing pressure. As compared with

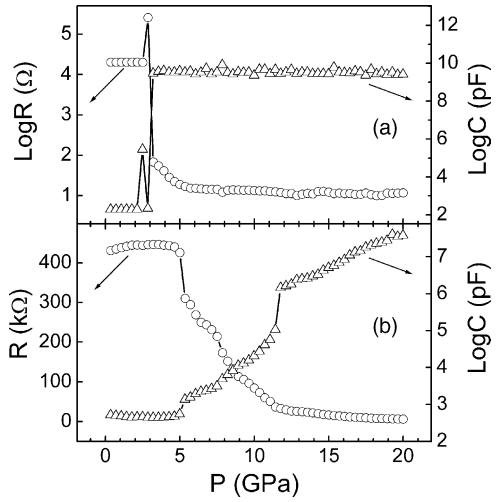

Fig. 5. The pressure dependence of resistance and capacitance for (a) Sr_2FeMoO_6 and (b) $Sr_2Fe_{1.4}Mo_{0.6}O_{6-\delta}$.

Sr_2FeMoO_6, the resistance of $Sr_2Fe_{1.4}Mo_{0.6}O_{6-\delta}$ (Fig. 5(b)) changes obviously at a higher pressure (5 GPa), with a slower decrease and within a wider range of pressure (5–11.8 GPa), and the capacitance of the sample varies in the same way except with a slower increase. Considering the results of energy dispersive X-ray diffraction, the abrupt drop of the resistance and the sharp increase of the capacitance for the two samples can be attributed to an electronic structural transition, which is caused by the compression of the unit cell under high pressure. These results are similar to those observed by Zhao et al. in Sr_2FeMoO_6 of μm scale grain size [13]. With the substitution of Fe for Mo, the change of the resistance and the capacitance for the sample becomes relatively tardy in a wider pressure range. A possible scenario to explain this behavior is that Fe substitution changes bond lengths and bond angles in the structure, which in turn change the band structure of the sample and results in a decrease of the sensitivity of the band structure to pressure. A more detailed study is in progress.

4. Conclusions

Iron-substituted products $Sr_2Fe_{1+x}Mo_{1-x}O_{6-\delta}$ ($x = 0$, 0.1, 0.2, 0.3, 0.4) can be synthesized by the modified polymer-network gel method at a relatively low temperature. All the samples, with grain sizes of about 100 nm, were indexed to a tetragonal structure with the space group I4/mmm. The in situ high pressure energy dispersive XRD results indicate that no crystal structural transition arises in the measured pressure range, showing that the structure of the samples is stable under high pressure. The bulk modulus, simulated from the B–M equation, suggests that the lattice of $Sr_2Fe_{1.4}Mo_{0.6}O_{6-\delta}$ is more compressible than that of the non-substituted sample Sr_2FeMoO_6. The steep drop of the *R–P* curve and the abrupt rise of the *C–P* curve within a definite pressure range are considered as being correlated to an electronic structural transition due to the compression of the unit cell under pressure which leads to a change of band structure. The relatively tardy change of the resistance versus pressure for $Sr_2Fe_{1.4}Mo_{0.6}O_{6-\delta}$ shows that Fe substitution produces some effect on the band structure.

Acknowledgements

This work was supported by the National Natural Science Foundation of China (No. 10274099, No. 50321101, and No. 50332020) and the State Key Development Project on Fundamental Research (No. 2002CB613301). We thank Professors L.C. Chen, Z.X. Bao and C.X. Liu for their help with the measurements.

References

[1] K.-I. Kobayashi, T. Kimura, H. Sawada, K. Terakura, Y. Tokura, Nature (London) 395 (1998) 677.
[2] T.H. Kim, M. Uehara, S.W. Cheong, S. Lee, Appl. Phys. Lett. 74 (1999) 1737.
[3] H. Han, B.J. Han, J.S. Park, B.W. Lee, S.J. Kim, C.S. Kim, J. Appl. Phys. 89 (2001) 7687.
[4] J. Linden, T. Yamamoto, J. Nakamura, H. Yamauchi, J. Appl. Phys. 78 (2001) 2736.
[5] Z. Fang, K. Terakura, J. Kanamori, Phys. Rev. B 63 (2001) 180407.
[6] K.-I. Kobayashi, T. Okuda, Y. Tomioka, T. Kimura, Y. Tokura, J. Magn. Magn. Mater. 218 (2000) 17.
[7] D. Sánchez, J.A. Alonso, M. García-Hernández, M.J. Martínez-Lope, J.L. Martínez, Phys. Rev. B 65 (2002) 104426.
[8] P.D. Battle, C.W. Jones, J. Solid State Chem. 78 (1987) 108.
[9] L.I. Balcells, J. Navarro, M. Bibes, A. Roig, B. Martinez, J. Fontcuberta, Appl. Phys. Lett. 78 (2001) 781.
[10] H.W. Zhang, S.Y. Zhang, B.G. Shen, C. Lin, J. Appl. Phys. 85 (1999) 4660.
[11] J.S. Zhang, H.J. Chen, J.H. Lin, J. Alloys Compd. 238 (2000) 113.
[12] Z.X. Bao, V.H. Schmidt, F.L. Howell, J. Appl. Phys. 70 (1991) 6804.
[13] P. Zhao, R.C. Yu, F.Y. Li, Z.X. Liu, J. Appl. Phys. 92 (2002) 1942.